NOTES AND CORRESPONDENCE

On the Representation of the 40–50 Day Oscillation in Terms of Velocity Potential and Streamfunction

JOHN E. GEISLER
Department of Meteorology, University of Utah, Salt Lake City, Utah

ERIC J. PITCHER*
Rosenstiel School of Marine and Atmospheric Science, University of Miami, Miami, Florida

16 June 1987 and 14 January 1988

1. Introduction

The 40–50 day oscillation was detected in tropical station data by Madden and Julian (1971, 1972) and interpreted as a pair of eastward propagating, overturning cells in the equatorial plane of the troposphere. Studies with a relatively simple dynamical model (Lau and Peng 1987) and with a general circulation model (Hayashi and Sumi 1986) support the idea that the 40–50 day oscillation consists of equatorially trapped modes forced by condensational heating. The analysis by Lorenc (1984) of the time series of velocity potential for observed 200 mb winds in the year of the Global Weather Experiment provides a different perspective. There, the 40–50 day oscillation appears as a zonal wavenumber-1 pattern extending from pole to pole. This raises the question of how or why an oscillation confined to the tropics should appear to have global meridional extent.

An essential step in reconciling this apparent paradox was recently made by Hendon (1986) in a note published in this journal. He derived the representation of a wavenumber-1 Kelvin wave in terms of its velocity potential and streamfunction. Figure 1 shows the result he obtained. Although the Kelvin wave, as defined by the meridional scale of its zonal velocity field (not shown), is trapped close to the equator, both the velocity potential and streamfunction exhibit patterns extending from pole to pole. The aspect which Hendon brought to light is that the divergent and nondivergent wind fields associated with the respective patterns shown in Fig. 1 exactly cancel outside a narrow strip near the equator. He further noted that the nondivergent wind is very much larger than the divergent wind close to the equator, a feature also apparent in Fig. 1.

Hendon suggested that it would be of interest to try to isolate in a global dataset a streamfunction pattern that would complement the global velocity potential pattern found by Lorenc (1984) in the manner shown in Fig. 1. With this objective in mind, we have analyzed a 1200-day record of a perpetual January simulation with a general circulation model. The purpose of this note is to present the result of that analysis.

2. Analysis procedure

The general circulation model is the NCAR Community Climate Model, version zero-A (CCM0A), a nine-level spectral model with rhomboidal truncation at wavenumber 15. The primary dataset consists of divergence and the vertical component of vorticity, archived twice daily. From these time series we calculated velocity potential and streamfunction, which were then averaged over nonoverlapping 5-day intervals through a 1200-day record from a perpetual January simulation with this model. The 1200-day means were removed to yield time series of anomalies.

We used the methodology developed by Lau and Lau (1986) as a basis for compositing the 5-day average anomalies in velocity potential and streamfunction. The first step was to obtain an empirical orthogonal function (EOF) representation of the unfiltered, global time series of 5-day average anomalies in velocity potential. Figure 2 shows the leading two EOFs. These represent 35% and 29% of the variance, respectively. A segment of the 1200-day record of the time series of the coefficients C_1 and C_2 for these two EOFs is shown in Fig. 3. These have been passed through the filter developed by Lau and Lau (1986), which has a bandpass of 16 to 45 days. The coefficients oscillate with a common frequency and are essentially 90° out of phase. In conjunction with the 90° spatial phase difference exhibited in Fig. 2, this temporal behavior signifies eastward propagation. To confirm that this regular behavior of the EOF coefficients is not a consequence of the bandpass filter, we examined power

* Present affiliation: Applications Department, Cray Research, Incorporated, Mendota Heights, MN 55120.

Corresponding author address: Dr. John E. Geisler, Dept. of Meteorology, The University of Utah, 819 Wm. C. Browning Bldg., Salt Lake City, UT 84112.

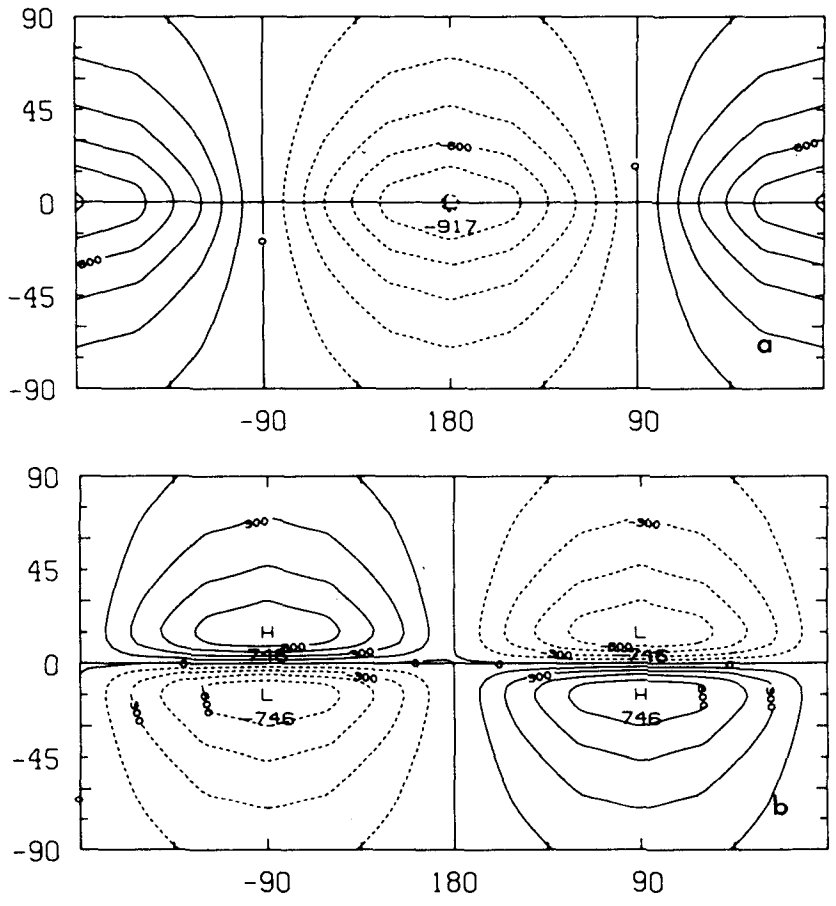

FIG. 1. (a) Velocity potential, and (b) streamfunction for a Kelvin wave of zonal wavenumber 1, phase speed 15 m s^{-1} (latitudinal Gaussian e-folding width $\approx 10°$) and amplitude of 1 m s^{-1}. Contour interval is 0.15×10^6 m^2 s^{-1}. [This figure has been reproduced from Hendon (1986).]

spectra of 200 mb velocity potential at points along the equator. In all cases the spectra exhibited pronounced peaks centered in the period range of 28 to 31 days. A representative example of these spectra was given in Pitcher and Geisler (1987). We have tested these peaks against a background red noise spectrum and found them to be significant at the 95% level.

We also examined the EOF representation of the unfiltered, global time series of 5-day average anomalies in streamfunction. Behavior analogous to that of EOFs 1 and 2 of velocity potential anomalies appeared in EOFs 2 and 3 of streamfunction anomalies, with the additional contrasting characteristic that the percent of variance accounted for was relatively small (6.7% and 6%, respectively). The pattern of EOF 1 of streamfunction anomalies, which accounted for 27% of the variance, was essentially zonally symmetric with maximum zonal wind along the equator.

The compositing in this study is done solely with reference to EOFs 1 and 2 of velocity potential anomalies. The temporal behavior of the coefficients C_1 and C_2 from Fig. 3 is shown in the form of a harmonic dial in Fig. 4. We assigned the individual 5-day average states, represented by the open circles, to one of the four categories defined by 90° wedges bisected by the axes labeled 1, 2, 3 or 4 in the figure. In the 1200-day record there are a total of 6 episodes similar to the one shown in Figs. 3 and 4, in which the relative phase of C_1 and C_2 is clearly defined and persistent over several cycles. We constructed harmonic dials (not shown) for all of these episodes and used them along with the one shown in Fig. 4 to composite the data from all well-defined episodes. The number of entries in the respective four categories is 15, 14, 15 and 22. From these harmonic-dial representations of the well defined episodes, we have obtained an estimate of 30 days for the period of the oscillation.

3. Results

The composite anomalies in categories 3 and 4 are similar and of opposite sign to those in categories 1 and 2. It is therefore sufficient to show only the two difference categories, 1–3 and 2–4. Velocity potential and streamfunction anomalies for these two difference categories are shown in Fig. 5. A zonal wavenumber-1 component in the streamfunction is readily discern-

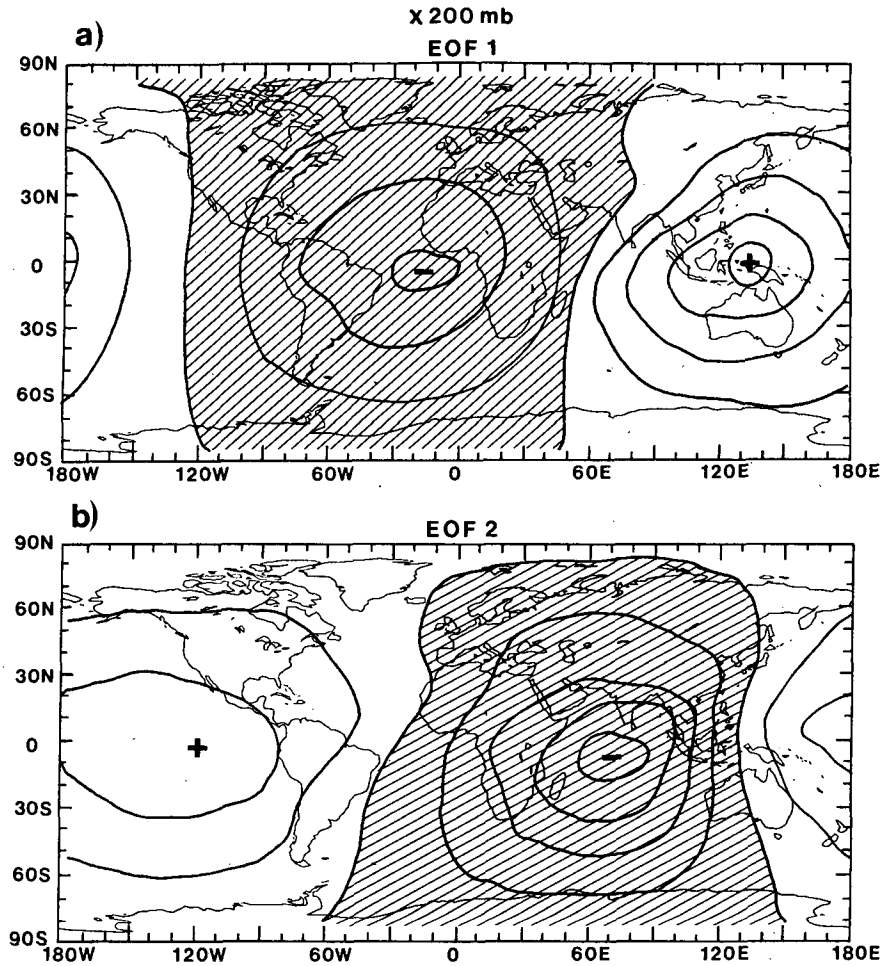

FIG. 2. (a) First, and (b) second empirical orthogonal functions (EOFs) for the global time series of 5-day-average anomalies in the 200 mb velocity potential. Units are arbitrary.

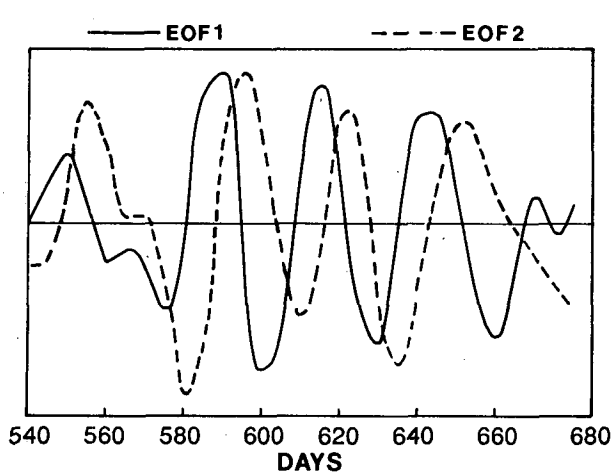

FIG. 3. A portion of the time series of bandpass (16–45 days) filtered coefficients for the EOFs shown in Fig. 2. Units are arbitrary.

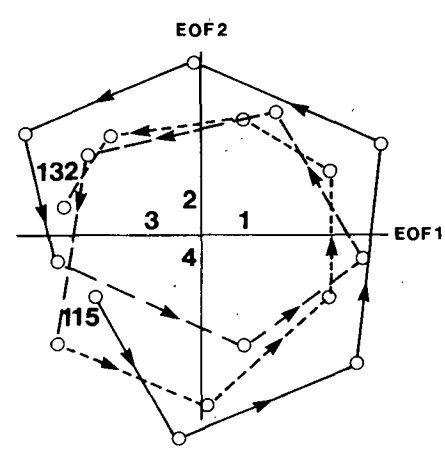

FIG. 4. Harmonic dial showing the temporal behavior of the EOF 1 and EOF 2 coefficients for the interval of time in Fig. 3. The counterclockwise phase progression indicates eastward propagation. Open circles represent points in the 240-member time series of 5-day averages. The integers on each axis denote the four compositing categories. First, second and third cycles of the oscillation are shown by a solid line, a long dash, and a short dash, respectively.

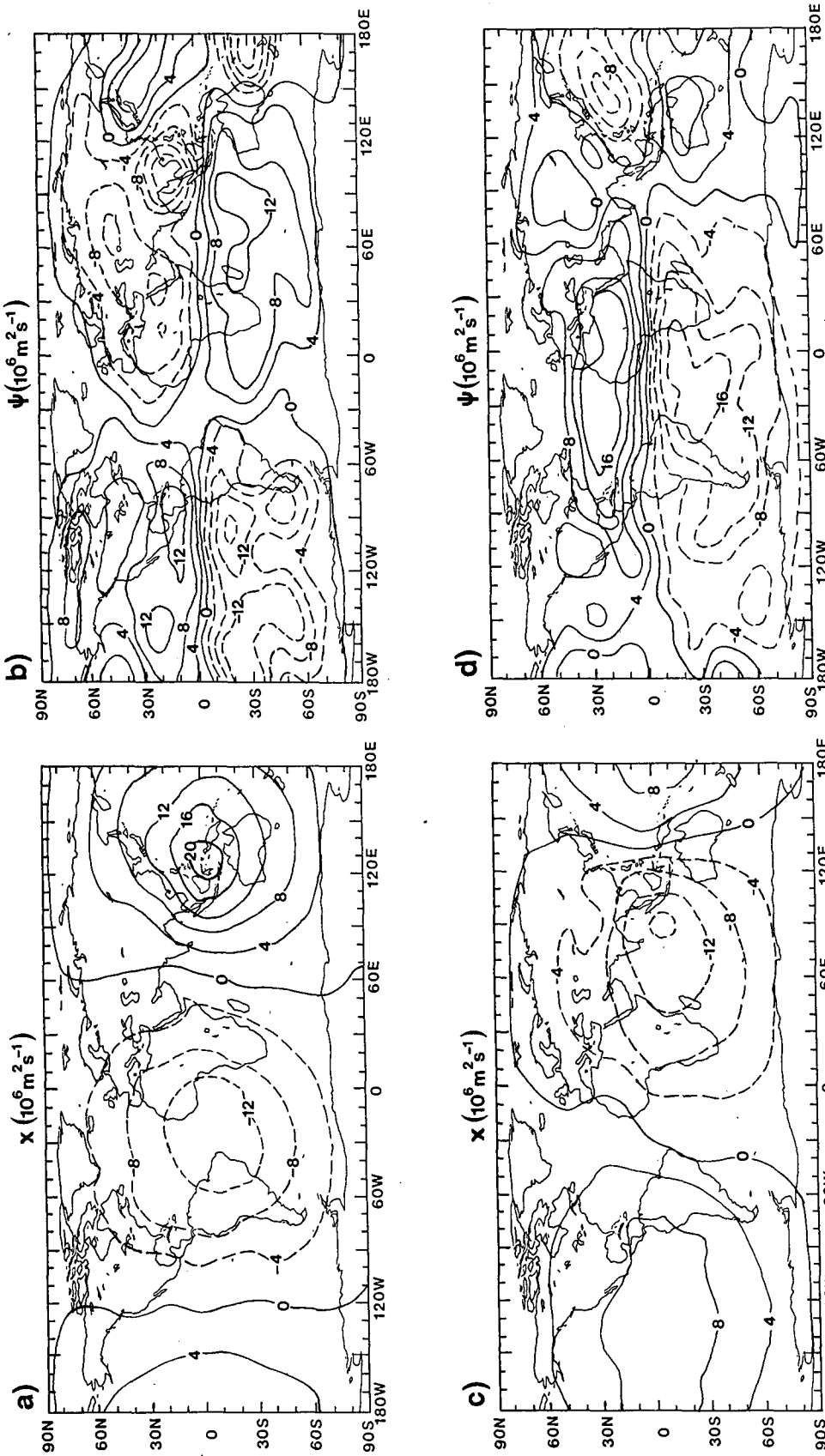

FIG. 5. (a) Velocity potential anomaly obtained by subtracting the category-3 composite from the category-1 composite (contour interval: 4×10^6 m^2 s^{-1}); (b) streamfunction anomaly obtained by subtracting the category-3 composite from the category-1 composite (contour interval: 4×10^6 m^2 s^{-1}); (c) As in (a), but for category-2 minus category-4; (d) As in (b), but for category 2 minus category 4.

ible and it is seen to bear the same phase relationship to the velocity potential pattern as that in Fig. 1. In category 1–3, for example, the node in the streamfunction (Fig. 5b) runs on the average along longitude 30°W, which is essentially the longitude of the velocity potential minimum in that category (Fig. 5a). It can be seen that in this category the nondivergent component of the meridional wind in the Atlantic sector of the globe opposes the divergent component. Reference to Fig. 5a also shows that the divergent component of the wind on the equator in category 1–3 is directed eastward from the Atlantic, across Africa and the Indian Ocean, and into the velocity potential maximum over Indonesia. It is reinforced along this trajectory by the nondivergent wind (Fig. 5b). Given that the contour interval is the same for both velocity potential and streamfunction, it can be estimated that the magnitude of the nondivergent wind along this equatorial trajectory is about a factor of 2 or 3 larger than the divergent wind.

In category 2–4 the velocity potential minimum has shifted eastward to the Indian Ocean (Fig. 5c). The nondivergent wind that runs westward across equatorial Africa and the Atlantic is about a factor of 4 larger than the divergent wind there.

The streamfunction pattern (Fig. 5b and 5d) in the East Asian sector of the Northern Hemisphere is so distorted by relatively small-scale circulation centers that the node is no longer oriented along a meridian. These circulation features bear some resemblance to those appearing in the composite life cycle of the oscillation that Knutson and Weickmann (1987) deduced from global wind analyses. For example, Fig. 5d shows that the approach to the dateline of a pair of cyclonic (anticyclonic) centers straddling the equator in category 2 (4) of the composite has the correct position to produce a modulation in the intensity and longitudinal extent of the climatological jet centered over the east coast of Asia in midlatitudes.

4. Discussion

By means of a compositing technique we have extracted from an extended simulation with a general circulation model an oscillation which appears in the velocity potential as a global oscillation, consisting primarily of zonal wavenumber 1 and propagating eastward with a period of ~30 days. The composite streamfunction pattern contains a global wavenumber-1 pattern of comparable amplitude having a quadrature relationship like that of the Hendon solution shown in Fig. 1. Composite studies using global datasets have not, to the authors' knowledge, revealed this aspect of the streamfunction pattern. In addition to this wavenumber-1 component, the streamfunction pattern exhibits smaller-scale circulation features that are not found in the velocity potential pattern. Thus, the exact cancellation of nondivergent and divergent wind that characterizes the Hendon solution in extratropical latitudes is not occurring in the simulated oscillation.

Representation in terms of velocity potential and streamfunction also suggests that the oscillation in the equatorial plane simulated here cannot be described simply as a pair of overturning cells, since the nondivergent component of zonal wind at 200 mb is typically a factor of 3 larger than the divergent component. The relative phase of these components is almost exactly one of quadrature, as inferred by the fact that the centers of velocity potential line up with the meridionally oriented nodes of the streamfunction. This characteristic of the simulated oscillation appears to be at variance with results obtained from analyses of global datasets. Knutson and Weickmann (1987) show that the relation between streamfunction and velocity potential is not one of simple quadrature throughout the life cycle of the oscillation. Their result is supported by Leibmann (1987), who obtained a positive temporal correlation between upper level zonal wind and outgoing longwave radiation anomalies, indicating that convection (hence, divergence) in the Indonesian sector occurs in easterlies.

Acknowledgments. This research was supported by the National Science Foundation under grants ATM8616370 and ATM8616371. This work has also been supported by the EPOCS Program of NOAA through a grant to the University of Miami. Acknowledgment for computing resources is made to the National Center for Atmospheric Research, which is supported by the National Science Foundation. The authors wish to acknowledge Klaus Weickmann and an anonymous reviewer for important suggestions.

REFERENCES

Hayashi, Y.-Y., and A. Sumi, 1986: The 30–40 day oscillations simulated in an "aqua planet" model. *J. Meteor. Soc. Jpn,* **64,** 451–467.

Hendon, H. H., 1986: Streamfunction and velocity potential representation of equatorially trapped waves. *J. Atmos. Sci.,* **43,** 3038–3042.

Knutson, T., and K. M. Weickmann, 1987: 30–60 day atmospheric oscillations: Composite life cycles of convection and circulation anomalies. *Mon. Wea. Rev.,* **115,** 1407–1436.

Lau, N. C., and K.-M. Lau, 1986: Structure and propagation of intraseasonal oscillations appearing in a GFDL GCM. *J. Atmos. Sci.,* **43,** 2023–2047.

Lau, K.-M., and L. Peng, 1987: Origin of the low frequency (intraseasonal) oscillations in the tropical atmosphere. *J. Atmos. Sci.,* **44,** 950–972.

Leibmann, B., 1987: Observed relationships between large-scale tropical convection and the tropical circulation on subseasonal time scales during the Northern Hemisphere winter. *J. Atmos. Sci.,* **44,** 2543–2561.

Lorenc, A. C., 1984: The evolution of planetary-scale 200 mb divergent flow during the FGGE year. *Quart. J. Roy. Meteor. Soc.,* **110,** 427–441.

Madden, R. A., and P. R. Julian, 1971: Detection of a 40–50 day oscillation in the zonal wind in the tropical Pacific. *J. Atmos. Sci.,* **28,** 702–708.

——, and ——, 1972: Description of global-scale circulation cells in the tropics with a 40–50 day period. *J. Atmos. Sci.,* **29,** 1109–1123.

Pitcher, E. J., and J. E. Geisler, 1987: The 40- to 50-day oscillation in a perpetual January simulation with a general circulation model. *J. Geophys. Res.,* **92,** 11,971–11,978.